

# Mechatronic Systems' Control Design Using Dynamic Emulation of Mechanical Loads

UDK 681.53  
IFAC 2.6.2;5.3.1

Original scientific paper

The paper presents and analyses rapid prototyping methods for the dynamic emulation of mechanical loads. Approaches can be applied in design, testing and validation of the mechatronic systems propelled by electric drives. Actual system (prototype) is replaced by the torque controlled electromechanical load, for which the required torque is calculated through the closed-loop control algorithm. The active load is connected mechanically to the drive shaft, using the clutch. Also possible applications in the control design for variable speed and torque drives are described. For the illustration of the method emulation of the pump mechanism is given.

**Key words:** mechatronic system, control design, dynamic emulation, mechanical load

## 1 INTRODUCTION

Modern companies strive to achieve a shorter time from the idea to the final product. Thus the time, available for the design is constantly shortened. In order to satisfy these demands the use of rapid prototyping approaches is gaining the importance in the design process.

Also the number of applications of variable speed and torque drives for the propelling of the mechanical systems has been increasing rapidly in last decades. Because of the growing complexity of the applications a demand for the improved development and testing equipment has occurred.

In many cases the operation of the electrical drives in the applications can not be tested on the actual system. This is frequently due to the fact, that it is either expensive or not available in the early phase of design. In order to test this critical component without the need for prototype various techniques were developed.

The classical approach, static emulation of mechanical loads, is performed using the torque-controlled dynamometer (Load Machine) acting as an active load [1, 2, 3, 4, 5]. Both machines – drive under test (Drive Machine) and dynamometer are connected mechanically, ideally with the common shaft, thus forming a Drive Machine – Load Machine (DM-LM) mechanism. The torque, applied by the Load Machine is calculated from speed and/or position of the rotor. This approach is successful in the emulation of mechanisms running with the constant or slowly changing speed.

Dynamic emulation of mechanical loads (DEML) presents an upgrade of this method, where with none or only minor changes in hardware it is possible to extend the use to the design of the variable speed and torque control algorithms. With the improved software algorithms it is successful also in the case of rapid speed and torque changes. It enables the testing of changing inertia and highly nonlinear dynamics. The torque applied by the Load Machine is calculated using the feedback control algorithm. Recent research, dealing with the dynamic emulation of mechanical loads [6, 7, 8] presented some useful approaches. However, they are mainly based on assumption, that the DM-LM mechanism dynamics is almost linear and well known.

In order to make the method applicable also to the DM-LM mechanisms exhibiting some nonlinear behavior, advanced methods were developed [9, 10]. They are based on nonlinear control approaches. Two methods are presented in the following text. First method uses the feedforward scheme calculating the inverse dynamics of the testing rig, compensating the unmodeled dynamics and parameter variations of the DM-LM mechanism, with the use of feedback PI controller. On the other hand, the second method (based on PI estimator) uses nonlinear control approach presented in [11], which makes it more robust towards impacts of parameter variations and unmodeled dynamics. Additionally the setting of poles is decoupled for the test-rig dynamics torque compensation and emulated model speed tracking.

Both methods are analyzed and also the calculation of their parameters is given. The operation is further presented with the use of experimental results, where nonlinear dynamics of the electrical pump mechanism's drive is emulated. Finally, comparison including advantages and disadvantages of both methods is presented.

Possible application is presented on the example of pump, driven by induction motor, where the practicability of the methods is presented with experimental results.

**2 DYNAMIC EMULATION OF MECHANICAL LOADS**

The basic idea of DEML is shown in Figure 1, where  $G$  is dynamics of the DM-LM mechanism and  $G_{em}$  is dynamics of the emulated mechanism.  $\omega_r$  is the rotor speed of the DM-LM mechanism,  $\omega_{em}$  the speed of the emulated mechanism,  $T_e$  the applied electrical torque of the Drive Machine, and  $T_L$  is the applied load torque of the experimental mechanism (Load Machine). Estimated values are denoted by  $\hat{\cdot}$ .

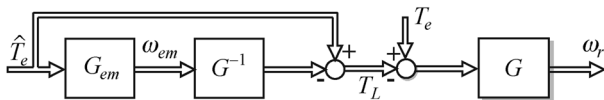


Fig. 1 Dynamic emulation of mechanical loads – basic idea

The transfer function of the DM-LM mechanism is presented with:

$$G(s) = \frac{1}{J_m s + B_m}, \tag{1}$$

and its estimation with:

$$\hat{G}(s) = \frac{1}{\hat{J}_m s + \hat{B}_m}, \tag{2}$$

where  $J_m$  is the inertia and  $B_m$  the viscous friction coefficient of the DM-LM mechanism.

The method uses the inverse model of the DM-LM mechanism, which is put in series (by the means of software) with the actual DM-LM mechanism. The input of the inverse model ( $\omega_{em}$ ) is calculated using the emulated system model.

If applied torque and all dynamic models are well known, complete system behaves in the same manner as the emulated mechanism would. However, because the inverse model of the DM-LM mechanism is usually not well known (varying parameters, unmodeled dynamics, external disturbances...), the method is not suitable for the practical use.

Therefore it is upgraded with the feedback controller. A method using the compensator was presented in [6, 7, 8]. The desired value of applied torque was used and because of the presence of compensator an additional delay occurs. New methods were developed in order to reduce the complexity of the load emulation algorithms.

They present improvements of the approach due to the fact, that the dynamics of the controller is not contained in the compensator, which enables the use of advanced non-linear control algorithms providing the compensation of non-linear friction. The DM-LM mechanism can be of lower quality, which results in reduced cost. The basic principle is described in Figure 2.

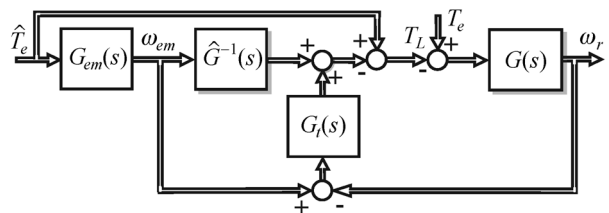


Fig. 2 Dynamic emulation of mechanical loads – basic principle

The desired value of speed  $\omega_{em}$  is obtained from the model of emulated mechanism. Feedback controller  $G_f$  is used for the compensation of unmodeled dynamics, parameter variations, and numerical errors.

The dynamic model of the emulated mechanism is presented in Figure 3 and (3), where  $\hat{T}_e$  is the estimated value of the applied torque,  $f_{em}$  is the emulated model friction,  $T_L^*$  is the additional load torque applied to emulated model, and  $J_{em}$  is the emulated model inertia.

$$G_{em}(s) = \frac{\omega_{em}(s)}{\hat{T}_e(s)} : \alpha_{em} = \frac{d\omega_{em}}{dt} = J_{em}^{-1}(\omega_{em})(T_e - T_L^* - f_{em}). \tag{3}$$

The calculation of the inverse dynamics of the emulated mechanism is not required. Additionally, since the emulated mechanism under consideration is presented as in Figure 3, the derivative of the emulated mechanism speed  $\alpha_{em}$  can also be directly obtained. The calculation of the inverse dynamics

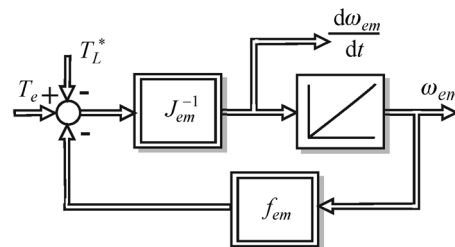


Fig. 3 Dynamic model of the emulated mechanism

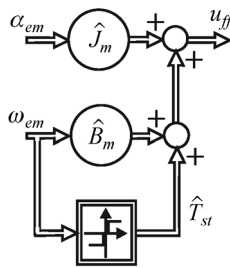


Fig. 4 Inverse dynamics -  $\hat{G}^{-1}$

of the DM-LM mechanism is presented in Figure 4, where  $T_{st}$  presents static (Coloumb) friction compensation torque.

### 3 APPROACH UTILIZING PI CONTROLLER

The setup of the method is presented in Figure 5. Nonlinear dynamics and torque estimation error are presented as input  $T_F$ . Estimated values are denoted by  $\hat{\cdot}$ , whereas desired values are denoted by  $d$ .

A well known PI controller, with parameters  $K_t$  and  $D_t$ , is used as the feedback controller  $G_t$ :

$$G_t(s) = K_t \frac{s + D_t}{s} \quad (4)$$

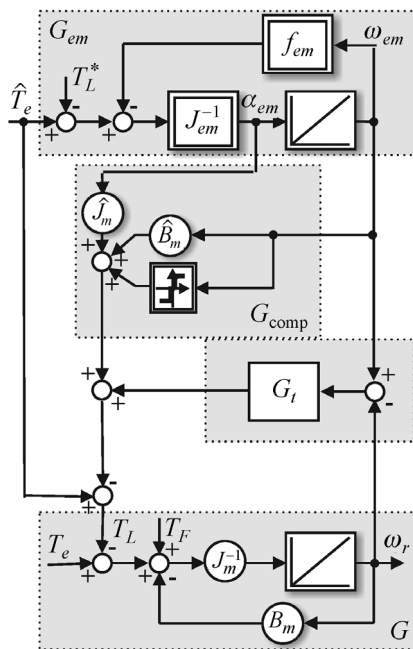


Fig. 5 Approach utilizing PI controller - Setup

#### A. Dynamic performance

Transfer function for speed is presented as:

$$\omega_r(s) = \frac{1 + G_t(s)\hat{G}(s)G(s)}{1 + G_t(s)G(s)\hat{G}(s)} \omega_{em}(s) + \frac{G(s)}{1 + G_t(s)G(s)} T_F(s) \quad (5)$$

After inserting (1), (2) and (4) into (5) we get:

$$\omega_r(s) = \frac{\hat{J}_m s^2 + (\hat{B}_m + K_t)s + K_t D_t}{J_m s^2 + (B_m + K_t)s + K_t D_t} \omega_{em}(s) + \frac{s}{J_m s^2 + (B_m + K_t)s + K_t D_t} T_F(s) \quad (6)$$

Bode plot describing the impact of unmodeled dynamics on speed is presented in Figure 6.

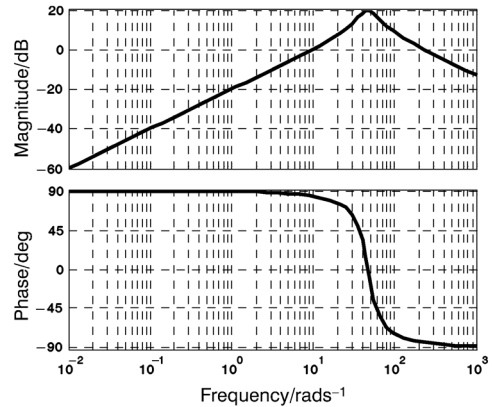


Fig. 6 PI controller - Bode plot -  $\omega_r/T_F$

#### B. Choice of parameters

Characteristic equation of the system is (based on (6)):

$$s^2 + \frac{B_m + K_t}{J_m} s + \frac{K_t D_t}{J_m} = 0 \quad (7)$$

If (7) is compared to the general equation of the 2<sup>nd</sup> order element:

$$s^2 + 2d\omega_0 s + \omega_0^2 = 0 \quad (8)$$

where  $d$  presents the damping and  $\omega_0$  the frequency of the 2<sup>nd</sup> order element, we get:

$$\omega_0^2 = \frac{K_t D_t}{J_m}, \quad 2d\omega_0 = \frac{B_m + K_t}{J_m} \quad (9)$$

Thus the values of parameters can be calculated as:

$$K_t = 2d\omega_0 J_m - B_m, \quad D_t = \frac{J_m \omega_0^2}{K_t} \quad (10)$$

#### C. Impact of parameter variations

In order to present the impact of parameter variations, influence of viscous friction coefficient is presented in Figure 7 ( $\hat{B}_m = 0.5 B_m$  - dashed line,  $\hat{B}_m = B_m$  - solid line,  $\hat{B}_m = 1.5 B_m$  - dotted line,  $\hat{B}_m = 2 B_m$  - dash-dot line).

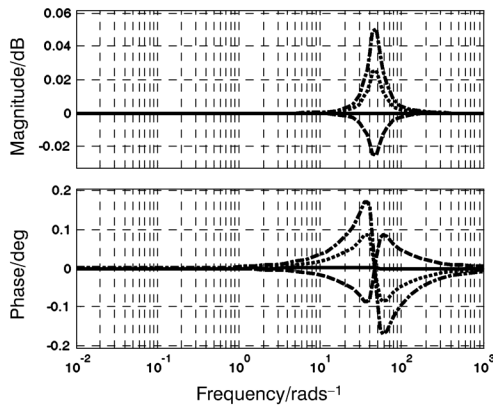


Fig. 7 PI controller – Bode plot –  $\omega_r/\omega_{em}$  – varying  $B_m$

The impact of the inertia variation is much greater. It is, however, possible to obtain the value of  $J_m$  with high precision for the testing mechanism.

**4 APPROACH UTILIZING PI ESTIMATOR**

The setup of the method is presented in Figure 8. PI estimator, as presented in [11], is used in combination with the state feedback controller.  $k$  is the feedback state controller gain and  $h$  is the PI estimator gain.

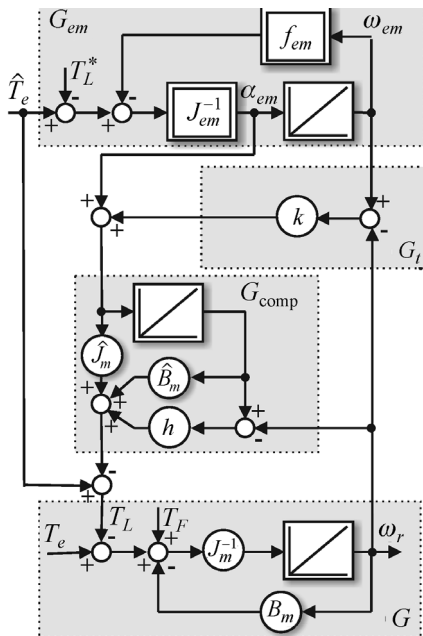


Fig. 8 Approach utilizing PI estimator – Setup

In the compensator the static friction compensation was not applied, which improves the robustness of the method to parameter variations and thus also its stability.

**A. Dynamic performance**

Transfer function of speed is presented as:

$$\omega_r(s) = \frac{\hat{J}_m s^2 + \hat{B}_m + h + \hat{J}_m k}{J_m s^2 + \frac{B_m + h + \hat{J}_m k}{J_m} s + \frac{k(\hat{B}_m + h)}{J_m}} \omega_{em}(s) + \frac{s}{J_m \left( s^2 + \frac{B_m + h + \hat{J}_m k}{J_m} s + \frac{k(\hat{B}_m + h)}{J_m} \right)} T_F(s), \tag{11}$$

which in ideal case, when  $\hat{J}_m = J_m$ ,  $\hat{B}_m = B_m$ , can be rewritten as:

$$\omega_r(s) = \omega_{em}(s) + \frac{s}{J_m \left( s + \frac{B_m + h}{J_m} \right) (s + k)} T_F(s). \tag{12}$$

Bode plot presenting the impact of unmodeled dynamics on speed is presented in Figure 9.

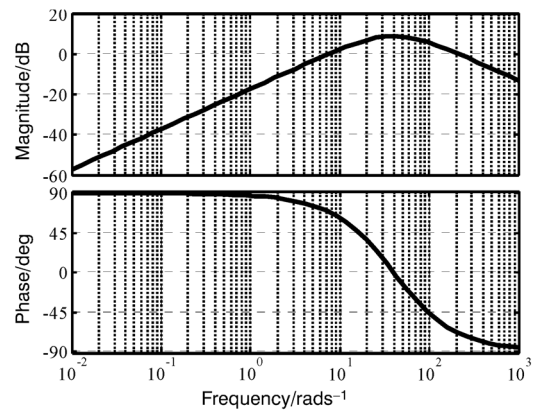


Fig. 9 PI estimator – Bode plot –  $\omega_r/T_F$

**B. Choice of parameters**

Characteristic equation of the system (based on (11)) is:

$$s^2 + \frac{B_m + h + \hat{J}_m k}{J_m} s + \frac{k(\hat{B}_m + h)}{J_m} = 0, \tag{13}$$

and can be rewritten as:

$$\left( s + \frac{\hat{B}_m + h}{J_m} \right) (s + k) = 0, \tag{14}$$

where it is assumed that  $B_m = \hat{B}_m$ . We get two real poles:

$$s_1 = -k, \quad s_2 = -\frac{\hat{B}_m + h}{J_m}, \tag{15}$$

from which two eigenvalues of the system can be calculated:

$$\omega_1 = k, \quad \omega_2 = \frac{\hat{B}_m + h}{J_m}, \quad (16)$$

and parameters can be calculated as:

$$k = \omega_1, \quad h = J_m \omega_2 - \hat{B}_m. \quad (17)$$

**C. Impact of parameter variations**

Like in the previous case, the impact of parameter variations is presented with the influence of viscous friction coefficient variation in Figure 7 ( $\hat{B}_m = 0.5 B_m$  – dashed line,  $\hat{B}_m = B_m$  – solid line,  $\hat{B}_m = 1.5 B_m$  – dotted line,  $\hat{B}_m = 2 B_m$  – dash-dot line).

As it was the case in the use of PI controller, the impact of the inertia variation is much greater. However, we again assume that the parameter is well known.

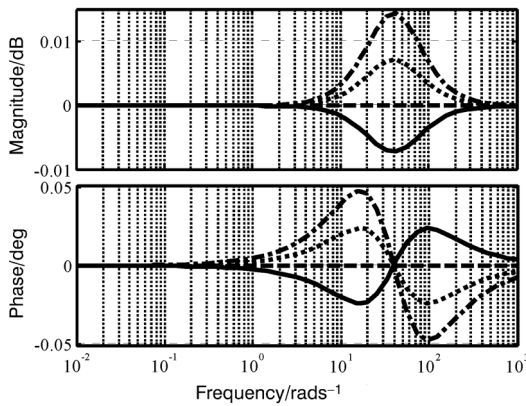


Fig. 10 PI estimator – Bode plot –  $\omega_r/\omega_{em}$  – varying  $B_m$

It can be observed from the Bode plots, that results are improved in the case of use of PI estimator. Especially the magnitudes are decreased, which shows the greater robustness to the impact of unmodeled dynamics and parameter variations. This is mainly due to the fact that it is simpler to set its parameters.

**5 EXPERIMENTAL RESULTS**

The experimental system is presented in Figure 11. Induction motor (Drive Machine) control is executed with the use of the dSPACE system containing DS1103 PPC controller board, and the Danfoss VLT5004 Inverter. The system is programmed with the use of MATLAB/Simulink. Measurements and computation of algorithm are exe-

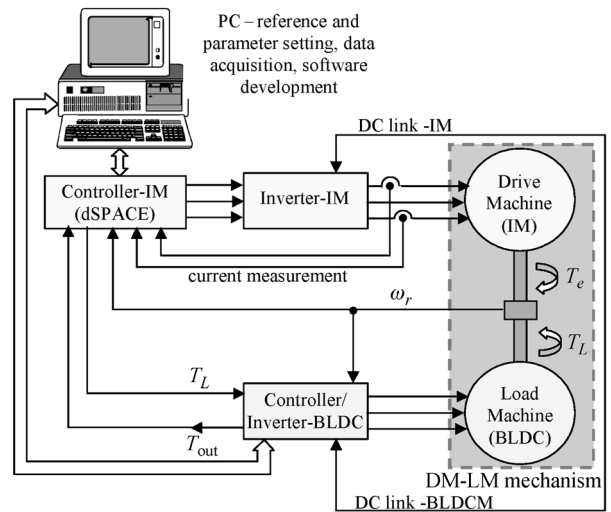


Fig. 11 Experimental system

cuted in 200  $\mu$ s. Brushless AC servomotor of type 142UMD400CACAA produced by UNIMOTOR driven by 7.5 kW Digital AC Drive UNI2402 (Uni-drive, Control Techniques) was used as the Load Machine. Both motors are mechanically connected using the clutch.

The dynamics of the simplified electric pump mechanism [12] is used as an example of the emulated dynamics. The system is presented in (18)–(19):

$$\frac{d\omega_{em}}{dt} = \frac{1}{J_p} \left( T_e - B_p \omega_{em} - K_{pp} \frac{Q h_p}{\omega_{em}} \right) \quad (18)$$

$$\begin{aligned} \frac{dQ}{dt} &= \frac{g A_p}{l_p} \left( h_p - (h_h - h_l) - \frac{k_{fp} l_p + k_l}{A_p^2} Q^2 \right) = \\ &= \frac{g A_p}{l_p} \left( (A_0 \omega_{em}^2 + B_0 \omega_{em} Q + C_0 Q^2) - \right. \\ &\quad \left. - (h_h - h_l) - \frac{k_{fp} l_p + k_l}{A_p^2} Q^2 \right). \quad (19) \end{aligned}$$

Where  $J_p$  is pump inertia,  $B_p$  is pump axis viscous friction,  $K_{pp}$  is load torque constant,  $A_0$ ,  $B_0$  and  $C_0$  are speed and throughput contribution coefficients.  $Q$  is the pump throughput and  $h_p$  is the pump head.  $k_{fp}$  is head loss coefficient due to the friction and  $k_l$  is local head loss coefficient. Pipe length is denoted by  $l_p$  and area with  $A_p$ , whereas  $h_h$  and  $h_l$  denote heights of the low- and high-end of the pipe, respectfully.  $g$  is gravity constant.

Experiments were executed with the use of speed control, where PI controller was used.

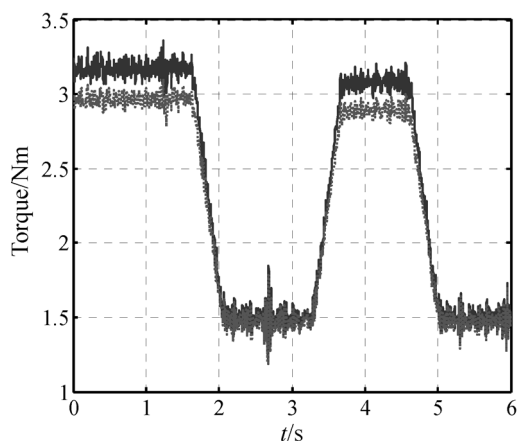


Fig. 12 PI controller – applied torque estimated ( $T_e$ , dotted line) and desired value ( $T_e^d$ , solid line)

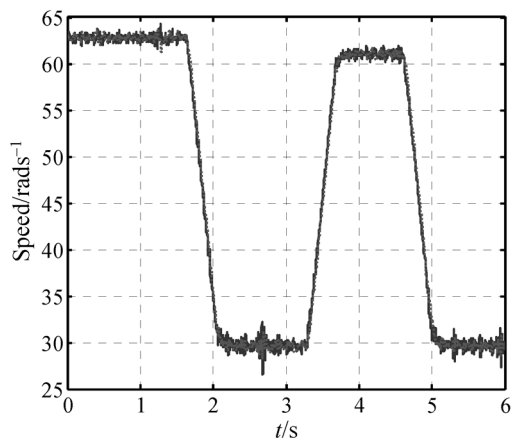


Fig. 13 PI controller – emulated ( $\omega_{emv}$ , dotted line) and actual ( $\omega_r$ , solid line) rotor speed

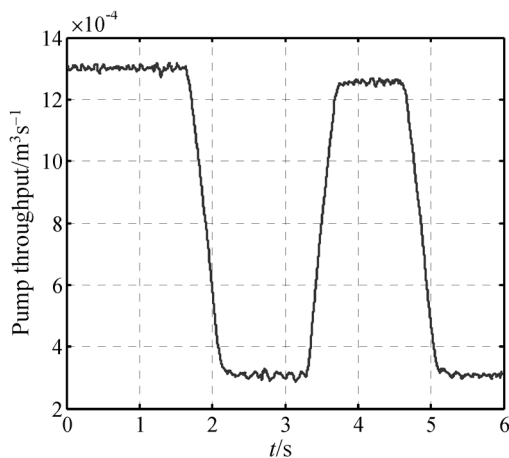


Fig. 14 PI controller – pump throughput ( $Q$ )

### A. PI controller

Results are presented in Figure 12 (applied torque estimated and desired value), Figure 13 (actual and emulated rotor speed), and Figure 14 (emulated pump throughput  $Q$ ).

Tracking of the torque controller is shown in Figure 12. It is not perfect. However the method, unlike the work of other authors ([6, 7, 8]) uses the estimated torque value for the calculation of the active load torque. Thus this case does not present a problem. Perfect tracking presented for the speed in the Figure 13. Thus the input/output behavior of the experimental system resembles the behavior of the drive machine with connected actual emulated load.

Torque control error increases with increasing speed, whereas speed error is not dependant on the values of the torque and speed. However, they are both increased at their rapid changes.

The operation of the emulated pump is additionally described by the presentation of the pump throughput  $Q$ , which changes with relatively high dynamics.

### B. PI estimator

Results for the applied PI estimator are presented in Figure 15 (applied torque estimated and desired value), Figure 16 (actual and emulated rotor speed), and Figure 17 (emulated pump throughput  $Q$ ).

Again, the tracking of the torque controller in the complete area of operation (Figure 15) is not perfect, but due to the fact that the method uses estimated value of the applied torque, this is not a problem. Good tracking is presented for the speed tracking in the Figure 16. Results are comparable

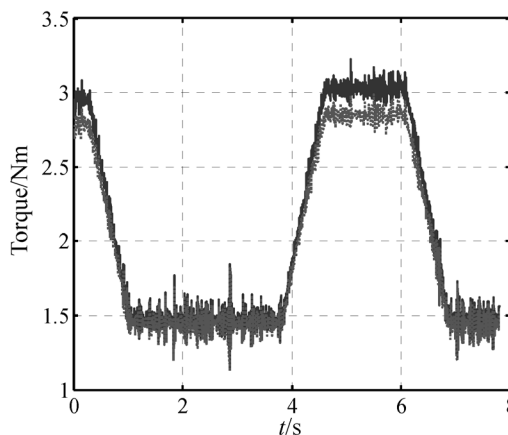


Fig. 15 PI estimator – applied torque estimated ( $T_e$ , dotted line) and desired value ( $T_e^d$ , solid line)

to the ones obtained by using a PI controller. Torque control error again increases with increasing speed, and so does the speed error. This shows the limitations of the method due to the applied algorithm's bandwidth. The PI estimator compensated the static friction of the testing mechanism, which at one point improves the stability and robustness of the method, but on the other hand reduces the bandwidth.

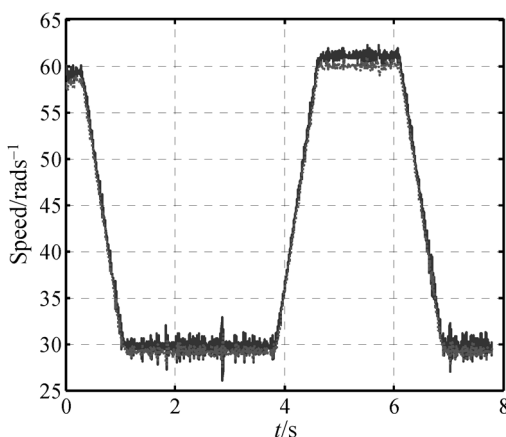


Fig. 16 PI estimator – emulated ( $\omega_{em}$ , dotted line) and actual ( $\omega_r$ , solid line) rotor speed

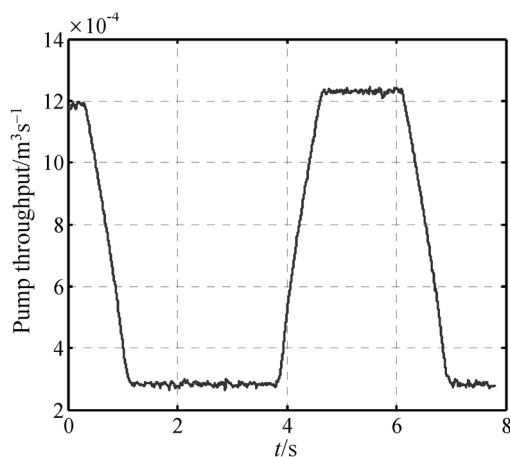


Fig. 17 PI estimator – pump throughput ( $Q$ )

The operation of the emulated pump is again improved by the presentation of the pump throughput  $Q$ , which also in this case changes with relatively high dynamics.

## 6 CONCLUSION

Without the need for the actual prototype, DEML methods enable the development of controllers

for various types of mechatronic components, operating at variable speed and torque.

In comparison to the classical methods (static load emulation), additional hardware is not required.

If two presented methods are compared, it can be observed that in the case of applied PI estimator the poles are real, which is not the case if PI controller is used. However, the use of PI estimator results in the simple setting of two independent parameters, whereas the parameters of PI controller are not independent.

The method applying PI estimator is easier to extend on the position control. Additionally, it enables the use of testing mechanisms with the dynamic model with the higher influence of non-linear effects (especially friction) and reduced precision of the mechanism parameters values.

## ACKNOWLEDGEMENT

The authors gratefully acknowledge the contributions of Ministry of Education, Science and Sport, Republic of Slovenia, for the financing of the work (project code: Z2-5349-796-03, Design and use of equipment for dynamic emulation of mechanical loads). We also thank to the government of Denmark, University of Alborg and Danfoss Company for the donation of equipment on which experiments were performed.

## REFERENCES

- [1] R. W. Newton, R. E. Betz, H. B. Penfold, **Emulating Dynamic Load Characteristic Using a Dynamic Dynamometer**. In Proceedings of the IEEE Power Electronics and Drive Systems (PEDS), Singapore, 1995, vol. 1, pp. 465–470.
- [2] C. R. Wasko, **500HP, 120 Hz Current-fed Field Oriented Control Inverter for Fuel Pump Test Stands**. In Conf. Rec. 1986 21<sup>st</sup> Annual Meeting IEEE Ind. App. Soc., pp. 314–320.
- [3] A. C. Williamson, **An Improved Engine-Testing Dynamometer**. In Fourth International Conference on Electrical Machines and Drives, IEE Conference Publication 310, 1989, pp. 374–378.
- [4] E. R. Collins, Y. Huang, **A Programmable Dynamometer for Testing Rotating Machinery Using Three-phase Induction Machine**. IEEE Trans. on Energy Conversion, vol. 9, 1994, pp. 521–527.
- [5] P. Sandholdt, E. Ritchie, J. K. Pedersen, R. E. Betz, **A Dynamometer Performing Dynamical Emulation of Loads with Non-linear Friction**. In Proceedings of the IEEE International Symposium on Industrial Electronics (ISIE'96), Warsaw, Poland, 1996, Part 2, pp. 873–878.
- [6] Z. H. Akpolat, G. M. Asher, J. C. Clare, **Dynamic Emulation of Mechanical Loads Using a Vector Controlled Induction Motor-Generator Set**. IEEE Trans. on Industrial Electronics, vol. 46, no. 2, 1999, pp. 370–379.
- [7] Z. H. Akpolat, G. M. Asher, J. C. Clare, **Experimental Dynamometer Emulation of Non-linear Mechanical Loads**.

- IEEE Trans. on Industry Applications, vol. 35, no. 6, 1999, pp. 1367–1373.
- [8] Z. H. Akpolat, G. M. Asher, J. C. Clare, **A Practical Approach to the Design of Robust Speed Controllers for Machine Drives**. IEEE trans. on Industrial Electronics, vol. 47, no. 2, 2000, pp. 315–324.
- [9] M. Rodič, K. Jezernik, M. Trlep, **A Feedforward Approach to the Dynamic Emulation of Mechanical Loads**. In Proceedings of the 35<sup>th</sup> Annual IEEE Power Electronics Specialists Conference (PESC'04), pp. 4595–4601, 2004.
- [10] M. Rodič, K. Jezernik, M. Trlep, **Feedforward and Feedback Approach for the Dynamic Emulation of Mechanical Loads**. In Proceedings of Symposium on power electronics, electrical drives, automation & motion: SPEEDAM 2004, Capry (Italy). pp. 555–560, 2004.
- [11] A. Hace, K. Jezernik, M. Terbuc, **VSS Motion Control for a Laser Cutting Machine**. Control Engineering Practice, Vol. 9, No. 1, 2001, pp. 67–77.
- [12] I. Elker, T. Kara, **Modelling and Simulation of Water Supply Systems for Feedback Control**. Rev. Energ. Ren.: Power Engineering (2001), pp. 49–55, 2001.

**Projektiranje upravljanja mehatroničkog sustava zasnovano na dinamičkom oponašanju mehaničkog tereta.** U članku se opisuje i analizira brza metoda dinamičkog oponašanja mehaničkog tereta. Pristup se može primijeniti za projektiranje, testiranje i provjeru valjanosti mehatroničkog sustava upravljanog elektromotornim pogonom, te posebno za prototipna ispitivanja. Aktualni sustav (prototip) je zamijenjen elektromehaničkim teretom, koji je upravljan momentom. Potrebni moment se računa iz zatvorene regulacijske petlje. Aktivni teret je spojkom mehanički povezan s pogonskom osovinom. Prikazane su također moguće primjene u projektiranju sustava promjenjive brzine i momenta. Za ilustraciju metode oponašanja tereta prikazan je pumpni mehanizam.

**Ključne riječi:** mehatronički sustav, projektiranje, dinamičko oponašanje, mehanički teret

#### AUTHORS' ADDRESSES

**M. Rodič**  
**K. Jezernik**  
**M. Trlep**

**Faculty of Electrical Engineering and Computer Science,  
 University of Maribor  
 Maribor, Slovenia**

Received: 2006-03-30